Published in final edited form as:
Calcif Tissue Int. 2013 June ; 92(6): 576–585. doi:10.1007/s00223-013-9720-z.

Effect of Zoledronate on the Responses of Osteocytes to Acute Parathyroid Hormone

Shinichiro Kuroshima, **Kirk William Elliott**, and **Junro Yamashita**
Department of Biologic and Materials Sciences, School of Dentistry, University of Michigan

Abstract

The bone anabolic effect of parathyroid hormone (PTH) therapy is blunted when used in patients who were previously on bisphosphonate treatment. Osteocytes may play a role in the bisphosphonate silencing effect on PTH therapy since bisphosphonates have been shown to reach the lacuno-canalicular system. *In vivo* osteocyte studies pose a significant challenge. For the current study, we developed a simple method to isolate RNA from the cortical bone enriched with osteocytes. Our purpose was to investigate how zoledronate (ZA) treatment modulates the responses of osteocytes and the bone marrow (BM) to an acute PTH treatment. Mice received ZA treatment for 3 months and a single PTH injection prior to euthanasia. Bone was histomorphometrically evaluated. Gene expression was assessed at the RNA level in osteocytes and BM. Endothelial progenitor cells (EPCs) and γδT-cells were analyzed in the BM and blood using flow cytometry. We found that ZA treatment altered bone responses to PTH. The expression of *sfrp4*, a Wnt antagonist, was significantly increased in ZA-affected osteocytes. BM EPCs were increased in response to acute PTH but not when treatment was combined with ZA. ZA treatment augmented EPCs in the BM but not in blood which suggests that ZA treatment may have differential effects between the BM and blood. These findings indicate that osteocytes and BM EPCs in mice on ZA treatment respond differently to acute PTH from those not receiving ZA. This may partially explain the mechanisms of previous reports that ZA therapy attenuates the anabolic effect of PTH in bone.

Keywords

Zoledronate; Osteocytes; PTH; endothelial progenitor cells; γδT-cells

Introduction

Nitrogen-containing bisphosphonates (N-BPs) and parathyroid hormone (PTH) are both approved for the treatment of osteoporosis but their mechanisms of actions are distinct. N-BPs suppresses bone turnover by suppressing resorption, while PTH stimulates bone turnover with a favor of bone formation over resorption [1]. Therefore, it is of interest whether combination therapy maximizes bone accrual. Clinical studies have demonstrated that the anabolic effect of PTH is blunted when used after N-BP treatment [2, 3], yet mechanisms of N-BPs silencing effect on PTH actions in bone are unclear.

Corresponding author: Dr. Junro Yamashita, 1011 North University Avenue, Ann Arbor, MI 48109-1078, Tel: 734-764-0238; Fax: 734-647-2110, yamashit@umich.edu.

Conflict of Interest: None

DISCLOSURES:
NONE

The authors have stated that they have no conflict of interest.

Osteocytes reside in mineralized matrix and interact with neighboring osteocytes via their long processes. N-BPs have an antiapoptotic effect on osteocytes in mice [4], while the long-term use of N-BPs may induce accumulated nonviable osteocytes in bone due to the suppression of bone remodeling [5]. Thus, N-BPs effects osteocyte cellularity but its clinical significance awaits clarification. Literature suggests that osteocytes are a key bone cell type in skeletal homeostasis by secreting crucial molecules that regulate mineral homeostasis [6]. Sclerostin, an inhibitor of the canonical Wnt pathway, is mainly produced by osteocytes [7]. Mutation of *SOST* that encodes sclerostin causes a high bone mass phenotype [8]. Mice with the osteocyte specific conditional inhibition of canonical Wnt signaling exhibit severe bone fragility [9], suggesting that the regulation of Wnt signaling in osteocytes is crucial for bone integrity. As mice with constitutively active parathyroid hormone (PTH) receptors in osteocytes exhibit elevated Wnt signaling and high bone mass [10], bone anabolism by PTH likely involves Wnt signaling in osteocytes. Thus, osteocytes are now acknowledged as a major therapeutic target for bone metabolic diseases. However, our understanding in osteocyte biology is limited because of their inaccessibility in the calcified matrix. In this study we investigated how ZA treatment influences the osteocytes' response to PTH *in vivo* using a newly developed method for isolating RNA from osteocytes in cortical bone.

Materials and Methods

Animals and *in vivo* injections

C57BL6 mice (9-week-old, n=88, females) were maintained in a temperature controlled room with a 12-hour light/dark cycle. Zoledronate (ZA) (Novartis, Stein, Switzerland) was administered subcutaneously for 3 months at 0.1mg/kg/week (n=44). An equivalent volume of vehicle (VC) was injected as control (n=44). A single injection of PTH at 80 μg/kg (Bachem, Torrence, CA) or saline was given to 36 mice in each group subcutaneously 30 minutes or 2 hours before euthanasia (Fig. 1). Neither a single injection of PTH nor saline was given to the remaining mice in each group before euthanasia. These doses were selected since the dose for rodent proof-of-concept studies is approximately 0.1 mg/kg/week for ZA [11–14] and 40~80 μg/kg/day for PTH [15, 16]. The protocol was approved and animals were treated in accordance with the guidelines of the University Committee on Use and Care of Animals.

Microcomputed tomography

The femurs were formalin-fixed and analyzed using microCT (Scanco Medical AG, Bruttisellen, Switzerland) to determine the effect of 3-month ZA treatment on the skeleton. The femurs were scanned at 10 μm voxel resolution. 300 cross-sectional slices were made at 10 μm intervals at the distal end beginning at the edge of the growth plate and extending in the proximal direction, and 100 contiguous slices starting 0.02mm proximal to the growth plate were selected for analysis of trabecular microarchitecture. The scans for midshaft cortical microarchitecture were obtained by 100 slices at the exact midpoint of the femur.

Histology

Tibiae were fixed, decalcified in 10% EDTA, embedded in paraffin, and processed for hematoxylin and eosin (H&E) and tartrate-resistant acid phosphatase (TRAP) staining. H&E staining was performed using a standard staining protocol. The Leukocyte Acid Phosphatase assay system (Sigma, St Louis, MO) was used for TRAP staining. The proximal metaphyseal region was histomorphometrically analyzed using Image-Pro Plus v4 (Media Cybernetics, Silver Spring, MD). The number of osteoclasts, total osteoclast surface per linear perimeter and osteoclast size were assessed. The osteoclast size was defined as the cell length in the direction parallel to the bone surface. Non-attached osteoclasts and $TRAP^+$ mononuclear cells (MNCs) were counted in the tibial BM within 100 μm of the bone

surface. $TRAP^+$ multinucleated cells that were not on the bone surface were considered non-attached osteoclasts as opposed to bone resorbing osteoclasts which were found on the bone surface.

Serum TRAcP5b and calcium

Serum was isolated from peripheral blood (PB) and kept at −80°C until use. Serum TRAP isoform 5b (TRAcP5b) levels were measured using the mouse TRAP assay (IDS, Boldon, UK). Serum calcium levels were determined using a commercially available kit (Pointe Scientific, Canton, MI).

RNA isolation from bone

At sacrifice, BM was isolated from the femur directly into TRIZOL (Invitrogen, Grand Island, NY) using centrifugation [13]. The BM sample was then homogenized, frozen in liquid nitrogen, and stored at −80°C before use. Femurs without the endosteum and periosteum were used to isolate osteocyte enriched RNA by scraping the endosteal surface of the femoral cortex using dental endodontic files (Dentsply, York, PA) to remove the adhered BM and lining cells. The scraped femoral cortex was frozen in liquid nitrogen and stored at −80°C. The cortex was then crushed into fine powder in liquid nitrogen. The bone powder was homogenized in TRIZOL and processed for RNA isolation. Total RNA was extracted by the phenol/chloroform method.

Quantitative real-time PCR

First-strand cDNA was synthesized using the SuperScript First-strand system (Invitrogen). Quantitative PCR (qPCR) was performed using an iCycler IQ (BioRad, Hercules, CA) with SYBR Green (Invitrogen). Samples were run in triplicate and results normalized to *18S* and *GAPDH* expression. Relative quantification of data generated using this system was performed using the standard curve method. Primers sets for the following genes were used: *Bim*, *BAD*, *BAK*, *Bcl2*, *MMP-13*, *Cxcl12*, *VEGFA*, *Sfrp4*, *S6K1*, *SOST*, *β-catenin*, *GSK3β*, and *mTOR* (Table 1).

Flow cytometry

BM was isolated from the right femurs and BM and blood were subjected to red blood cell lysis. MNCs (1×10^6) were incubated with a combination of fluorescein isothiocyanate (FITC) anti-mouse CD34, phycoerythrin (PE) anti-mouse VEGFR2, and allophycocyanin (APC) anti-mouse CD133. MNCs were also incubated with PE anti-mouse δγTCR. FITC Rat IgG2a, PE Rat IgG2a, APC Rat IgG2b, and APC Rat IgG1 were used for isotype controls. Cell analyses of $CD34^+$, $VEGFR2^+$, $CD133^+$, and $\delta\gamma TCR^+$ were performed using the C6 Flow Cytometer (BD Accuri Cytometers, Ann Arbor, MI). Antibodies were purchased from eBioscience (San Diego, CA).

Statistics

Independent *t*-tests for two groups and ANOVA for multiple groups were performed for parametric data. Tukey's test was used as a post hoc test. All statistical analysis was conducted with SYSTAT 12 (Systat software Inc., Chicago, IL). An α-level of 0.05 was used. Results are presented as mean ± standard error.

RESULTS

ZA treatment increased non-attached osteoclasts

MicroCT analysis of the distal femurs showed that the ZA-treated mice exhibited significantly more trabecular bone than vehicle control (Fig. 2A and Table 2). Tissue

mineral density (TMD) of trabecular bone was significantly higher in the ZA-treated mice compared to VC. ZA treatment affected the cortical bone as well. The cortex of the mid-femurs was thicker and denser in the ZA-treated mice than VC. Osteoclast surfaces and numbers per linear perimeters in the ZA group were significantly smaller than those in VC. Thus, 3-month ZA treatment exerted the expected antiresorptive effect in bone, resulting in significantly higher bone mass as compared to VC. Interestingly, the size of osteoclasts on the bone surface was significantly larger in the ZA than VC group. We further counted the numbers of non-attached osteoclasts and $TRAP^+$ MNCs in the tibial BM within 100 μm of the bone surface. The $TRAP^+$ multinucleated cells and MNCs were predominantly found in the BM nearby (but not on) the bone surface (Fig. 2B). In the ZA group, significantly greater numbers of non-attached osteoclasts and $TRAP^+$ MNCs were noted compared to VC. Serum TRAcP5b levels in the ZA-treated mice were significantly lower than in control despite the significant increase in the numbers of non-attached osteoclasts and $TRAP^+$ MNCs in the bone marrow.

Osteocyte dominant RNA isolation from the femoral cortex

We developed a simple method to isolate total RNA from the cortical bone. The photomicrograph of H&E-stained section of tibia where the BM was flushed multiple times with phosphate buffered saline exhibited discernible remnants of trabecular bone, BM cells, ant the endosteum (Fig.3A top), while the tibia in which the endosteal and periosteal surfaces were mechanically scraped showed minimal residual BM cells (Fig. 3A bottom). Thus, nearly all BM cells and endosteum were removed from the cortical bone with this novel filing method. To confirm that RNA isolated from the filed cortical bone was derived from essentially osteocytes, genes expressed particularly in osteocytes were assessed (*SOST*). Also, *cxcl12* was assessed as it is mainly expressed in BM cells. As shown in Fig. 3B, the expression of *SOST* was significantly higher in the cortex than the BM. The expression of *cxcl12* was significantly lower in the filed bone but not in the flushed bone, showing that the filing method removed the majority of BM cells and the endosteum. These results indicate that RNA isolated from the filed cortical bone was osteocyte dominant RNA.

ZA treatment altered calcium homeostasis in response to acute PTH

Serum calcium levels significantly increased in response to acute PTH in VC, confirming systemic PTH effects in mice [17] (Fig. 3C). However, the ZA-treated mice did not respond to acute PTH as the VC mice did; no differences were noted in the serum calcium levels between the PTH-injected and saline-injected mice. When the ZA mice receiving a saline injection were compared to the VC mice receiving a saline injection, ZA treatment significantly reduced the serum calcium levels. Thus, 3-month ZA treatment decreased serum calcium levels and blunted the calcium response to acute PTH.

Osteocyte response to acute PTH in ZA-treated mice

The responses of osteocytes to acute PTH were investigated at the RNA level. When the mice with neither PTH nor saline single injection prior to euthanasia were compared between the ZA and VC groups, significantly reduced expression of *β-catenin* was observed in the ZA-treated mice (Fig. 4A). However, no statistical differences were noted in other genes studied here between the ZA and VC groups. A single injection of PTH significantly downregulated the expression of *S6K1* at 2 hours in both the VC- and ZA-treated mice (Fig. 4B). Significantly elevated expression of *sfrp4* in response to acute PTH at 2 hours was noted in the ZA-treated mice but not in VC group.

Bone marrow response to acute PTH in ZA-treated mice

When mice with neither PTH nor saline single injection prior to euthanasia were compared between the ZA and VC groups, significantly increased expression of *Bim, BAD, Bcl2*, and *VEGFA* was observed in the ZA-treated mice (Fig. 5A). In the VC mice, acute PTH stimulated the expression of *Bcl2* at 30 minutes, and *Bim* and *MMP-13* at 2 hours (Fig. 5B). However, in the ZA-treated mice, *MMP-13* was the only gene which was significantly induced by acute PTH.

Differential impact of ZA in bone marrow and peripheral blood

The effect of acute PTH at 2 hours was assessed in the BM and PB of the VC- and ZA-treated mice. When the ZA-treated mice receiving a saline injection were compared to the VC-treated mice receiving a saline injection, ZA treatment significantly increased the percent of endothelial progenitor cells (EPC: $CD34^+CD133^+VEGFR2^+$) in the BM but had no effect in PB (Fig. 6A and 6B). The percent of BM EPCs was significantly increased in response to acute PTH in the VC-treated mice, while in the ZA-treated mice, a non-significant decrease was noted (Fig. 6A). However, acute PTH had not significant effect on PB EPC in both VC- and ZA-treated mice (Fig. 6B). The percent of γδT-cells did not change significantly in the BM of both VC- and ZA-treated mice in response to acute PTH (Fig. 6C). However, in PB, acute PTH significantly decreased the percentage of γδT-cells in the VC-treated mice, but not in the ZA-treated mice (Fig. 6D). These results indicate that ZA treatment elicited a differential effect in BM vs. PB.

Discussion

It has been reported that the bone anabolic effect of PTH is blunted when applied to osteoporotic patients who have been on N-BP therapy [2, 3]. The mechanisms of this blunted PTH effect by N-BPs are unclear. This study was designed to determine the mechanisms by which previous N-BP treatment undermines the bone anabolism of PTH therapy at the osteocyte level. Literature shows that osteoporosis is associated with increased osteocyte apoptosis [18]. However, little is known about the effect of bisphosphonates on osteocytes due to their inaccessibility in the calcified matrix. Bisphosphonates circulate in plasma for a few hours after administration with the majority binding to trabecular bone, however some reaches the lacuno-canalicular system [19]. As osteocytes reside in the lacuno-canalicular system for years and have the ability to reshape the peri-lacunar matrix [20], osteocytes are likely affected by bisphosphonates. In this study, we developed a simple method to isolate osteocyte-dominant RNA from the dense cortical bone and confirmed that the method indeed works by observing a high level of osteocyte-associated *SOST* and a low level of BM-associated *cxcl12* expression. To characterize the osteocytes in our model, acute PTH administration was given to the ZA-treated mice. Literature reports that the chronic elevation of PTH downregulates *SOST* and activates the Wnt pathway in osteocytes [10, 21] and that PTH protects osteocytes from apoptosis [22]. Hence, in this study we examined genes related to Wnt signaling and apoptosis. Without an acute injection, no significant differences were noted in the gene expression of osteocytes except *β-catenin* between the mice on ZA vs. VC. However, osteocytes' responses to acute PTH were different. In the ZA-affected osteocytes, acute PTH significantly increased the expression of *sfrp4* at 2 hours. As the protein product of *sfrp4* decreases bone formation by abating the Wnt pathway [23], the increased *sfrp4* suggests that ZA treatment might have an impact on osteocytes by attenuating PTH-activated Wnt signaling. We expected the downregulation of *SOST* with acute PTH, but no change in the expression of *SOST* was observed in this study. Bellido et al, reported that while continuous PTH downregulated *SOST*, intermittent PTH did not affect *SOST* in osteocytes, and that a single injection of PTH transiently suppressed *SOST* but this was observed only after the first injection [21]. The inconsistency between

their finding and our result could be due to a difference in the bone used for analysis. We used the filed dense cortical bone which is free from BM cells, endosteum, and periosteum. On the other hand, Bellido's group used the lumber vertebra which is primarily composed of trabecular bone including the bone marrow. As sclerostin is found not only in osteocytes but also a small amount in osteoblasts and osteoclasts [24, 25], their results might be influenced by the *SOST* expression in other cell types as well as osteocytes. In the BM, ZA treatment alone significantly upregulated *Bim, BAD, Bcl2,* and *VEGFA*. Acute PTH upregulated *Bcl2* and *Bim* in the VC-treated mice but such upregulation was not observed in the ZA-treated mice. Thus, BM cells were influenced by 3-month ZA treatment. As BM is a heterogeneous cellular environment, it is not known which specific cell types are responsible for this increase, however, it may reflect the increased non-attached osteoclasts and $TRAP^+$ MNCs. These findings may give an empirical explanation for the silencing effect of N-BPs on PTH therapy since osteocytes are known to play a major role in PTH-induced bone anabolism [22].

When mice with a single saline injection were compared between VC and ZA, the percentage of EPCs per total MNCs was different between the BM and PB. 3-months ZA treatment significantly increased EPCs in the BM. It has been proposed that ZA treatment has an anti-angiogenic property and suppresses EPCs [26]. Contrarily, N-BPs are used to treat avascular osteonecrosis of the femoral head with promising outcomes, suggesting that ZA treatment may not interfere with vascularization [27]. Thus, our finding that ZA treatment for 3 months significantly increases BM EPCs supports BPs' therapeutic effect in avascular osteonecrosis of the femoral head. As the bone anabolic effect of PTH has been linked to increased angiogenesis [28], in this study we assessed whether ZA treatment alters the number of EPCs in response to acute PTH. It has been demonstrated that PTH induced significant changes in gene expression of BM cells at 1 hour post-administration [17]. Hence, the EPC levels at 2 hours post-injection were assessed in the BM and PB. Interestingly, acute PTH significantly expanded EPCs in the BM of the VC-treated mice, while such an immediate effect was attenuated in the ZA-treated mice, indicating that 3-month ZA treatment altered the response of the BM to acute PTH. Taken together with the increased expression of *sfrp4* in ZA-affected osteocytes, these findings may support the blunted PTH anabolic actions in bone following bisphosphonate treatment.

It has been demonstrated that the number of circulating γδT-cells was greatly reduced by N-BP treatment and such a reduction was long-lasting, even after cessation of the treatment [29, 30]. Since N-BPs modulate the number of circulating γδT-cells, which is associated with acute phase reaction [31], we assessed γδT-cell levels in the PB and BM to confirm the effect of ZA treatment and their responses to acute PTH. In PB with acute saline, we saw a non-significant decrease in the γδT-cell level with ZA, which is in line with previous findings [29, 30]. Interestingly, acute PTH significantly decreased γδT-cells in the PB of the VC-treated mice but not in the ZA-treated mice. The biological significance of the suppressive effect of acute PTH on γδT-cells in PB is unknown.

In this study, 3-month ZA treatment indeed suppressed bone resorption significantly. Although osteoclasts were suppressed in mice on ZA vs. VC treatment, it was interesting to note that the size of osteoclasts in mice on ZA treatment was significantly larger than in VC. Furthermore, significantly more numbers of non-attached osteoclasts and $TRAP^+$ MNCs, located near but not on the bone surfaces, were noted in mice on ZA treatment vs. control. These findings were similar to a report by Weinstein et al. where increased numbers of giant and non-attached osteoclasts were observed in bone-biopsy specimens from patients on N-BP treatment [32]. When bone resorption occurs, N-BPs are internalized and inhibit the prenylation of small GTPases, resulting in osteoclast disintegration [33]. Though the inhibition of protein prenylation may eventually lead to osteoclast apoptosis, it could simply

interfere with osteoclasts' attachment to the bone since apoptosis is secondary for the antiresorptive effect of N-BPs [34]. This may account for the observation of non-attached osteoclasts predominantly seen near the bone surfaces in the ZA-treated mice. The significance of the increased numbers of non-attached osteoclasts in ZA-treated mice is currently unknown. As osteoclasts were suppressed significantly, decreased osteoblast surface was anticipated due to the coupling of bone resorption and formation. However, osteoblasts were not suppressed in this study. The probable explanation is that the 9-week-old mice used in the study were still in the growing stage where bone formation exceeds resorption [35]. Hence, a coupling effect could be masked and not clearly detected.

The analysis of signaling molecules was only performed at the RNA level, not at the protein level in this study. This is due to technical difficulties in the isolation of osteocyte protein from the cortex and a weakness of the study. The altered Wnt signaling in ZA-affected osteocytes in response to PTH *in vivo* needs to and could be verified using genetic approaches in future studies. ZA was administered at 0.1 mg/kg in this study. Using a dose conversion table between different species recommended by Center for Drug Evaluation and Research at the FDA [36], our dose of 0.1 mg/kg/w corresponds to approximately 2.2 mg/month (26.4mg/year) in human adults. Since ZA is administered at 4mg every 3~4 weeks in human for the treatment of bone metastatic diseases, our subcutaneous dose is considered safe nonetheless effective to stimulate bone cells. However, when compared to the ZA dose for the management of osteoporosis (5mg/year), our dose is considerably high. The clinical relevance of the results, therefore, needs to be interpreted with caution.

In summary, using our novel RNA isolation technique specific for osteocytes, we found that PTH administration exerted a differential effect on the expression of *Sfrp4* in osteocytes depending on the previous history of ZA treatment; PTH excited osteocytes to express *Sfrp4* in ZA-treated mice but not in control. The antiapoptotic effect of PTH was also blunted in osteocytes of ZA-treated mice. Data presented here may partially explain the mechanisms of previous reports that ZA therapy attenuates the anabolic effect of PTH in bone.

Acknowledgments

This study was supported by the NIH/NIDCR grant (R03DE018923). The microCT Core facility was funded partly by NIH/NICRR grant (S10RR026475-01).

References

1. Dempster DW, Zhou H, Recker RR, Brown JP, Bolognese MA, Recknor CP, Kendler DL, Lewiecki EM, Hanley DA, Rao DS, Miller PD, Woodson GC 3rd, Lindsay R, Binkley N, Wan X, Ruff VA, Janos B, Taylor KA. Skeletal histomorphometry in subjects on teriparatide or zoledronic acid therapy (SHOTZ) study: a randomized controlled trial. J Clin Endocrinol Metab. 2012; 97:2799–2808. [PubMed: 22701017]
2. Ettinger B, San Martin J, Crans G, Pavo I. Differential effects of teriparatide on BMD after treatment with raloxifene or alendronate. J Bone Miner Res. 2004; 19:745–751. [PubMed: 15068497]
3. Obermayer-Pietsch BM, Marin F, McCloskey EV, Hadji P, Farrerons J, Boonen S, Audran M, Barker C, Anastasilakis AD, Fraser WD, Nickelsen T. Effects of two years of daily teriparatide treatment on BMD in postmenopausal women with severe osteoporosis with and without prior antiresorptive treatment. J Bone Miner Res. 2008; 23:1591–1600. [PubMed: 18505369]
4. Plotkin LI, Bivi N, Bellido T. A bisphosphonate that does not affect osteoclasts prevents osteoblast and osteocyte apoptosis and the loss of bone strength induced by glucocorticoids in mice. Bone. 2011; 49:122–127. [PubMed: 20736091]
5. Allen MR, Burr DB. Mandible matrix necrosis in beagle dogs after 3 years of daily oral bisphosphonate treatment. J Oral Maxillofac Surg. 2008; 66:987–994. [PubMed: 18423290]

6. Xiong J, Onal M, Jilka RL, Weinstein RS, Manolagas SC, O'Brien CA. Matrix-embedded cells control osteoclast formation. Nat Med. 2011; 17:1235–1241. [PubMed: 21909103]
7. Poole KE, van Bezooijen RL, Loveridge N, Hamersma H, Papapoulos SE, Lowik CW, Reeve J. Sclerostin is a delayed secreted product of osteocytes that inhibits bone formation. Faseb J. 2005; 19:1842–1844. [PubMed: 16123173]
8. Balemans W, Ebeling M, Patel N, Van Hul E, Olson P, Dioszegi M, Lacza C, Wuyts W, Van Den Ende J, Willems P, Paes-Alves AF, Hill S, Bueno M, Ramos FJ, Tacconi P, Dikkers FG, Stratakis C, Lindpaintner K, Vickery B, Foernzler D, Van Hul W. Increased bone density in sclerosteosis is due to the deficiency of a novel secreted protein (SOST). Hum Mol Genet. 2001; 10:537–543. [PubMed: 11181578]
9. Kramer I, Halleux C, Keller H, Pegurri M, Gooi JH, Weber PB, Feng JQ, Bonewald LF, Kneissel M. Osteocyte Wnt/beta-catenin signaling is required for normal bone homeostasis. Mol Cell Biol. 2010; 30:3071–3085. [PubMed: 20404086]
10. O'Brien CA, Plotkin LI, Galli C, Goellner JJ, Gortazar AR, Allen MR, Robling AG, Bouxsein M, Schipani E, Turner CH, Jilka RL, Weinstein RS, Manolagas SC, Bellido T. Control of bone mass and remodeling by PTH receptor signaling in osteocytes. PLoS One. 2008; 3:e2942. [PubMed: 18698360]
11. Croucher PI, De Hendrik R, Perry MJ, Hijzen A, Shipman CM, Lippitt J, Green J, Van Marck E, Van Camp B, Vanderkerken K. Zoledronic acid treatment of 5T2MM-bearing mice inhibits the development of myeloma bone disease: evidence for decreased osteolysis, tumor burden and angiogenesis, and increased survival. J Bone Miner Res. 2003; 18:482–492. [PubMed: 12619933]
12. Yaccoby S, Pearse RN, Johnson CL, Barlogie B, Choi Y, Epstein J. Myeloma interacts with the bone marrow microenvironment to induce osteoclastogenesis and is dependent on osteoclast activity. Br J Haematol. 2002; 116:278–290. [PubMed: 11841428]
13. Yamashita J, Koi K, Yang DY, McCauley LK. Effect of zoledronate on oral wound healing in rats. Clin Cancer Res. 2011; 17:1405–1414. [PubMed: 21149614]
14. Kuroshima S, Go VA, Yamashita J. Increased Numbers of Nonattached Osteoclasts After Long-Term Zoledronic Acid Therapy in Mice. Endocrinology. 2012; 153:17–28. [PubMed: 22109892]
15. Jacome-Galarza CE, Lee SK, Lorenzo JA, Aguila HL. Parathyroid hormone regulates the distribution and osteoclastogenic potential of hematopoietic progenitors in the bone marrow. J Bone Miner Res. 2011; 26:1207–1216. [PubMed: 21611963]
16. Bedi B, Li JY, Tawfeek H, Baek KH, Adams J, Vangara SS, Chang MK, Kneissel M, Weitzmann MN, Pacifici R. Silencing of parathyroid hormone (PTH) receptor 1 in T cells blunts the bone anabolic activity of PTH. Proc Natl Acad Sci U S A. 2012; 109:E725–733. [PubMed: 22393015]
17. Li X, Liu H, Qin L, Tamasi J, Bergenstock M, Shapses S, Feyen JH, Notterman DA, Partridge NC. Determination of dual effects of parathyroid hormone on skeletal gene expression in vivo by microarray and network analysis. J Biol Chem. 2007; 282:33086–33097. [PubMed: 17690103]
18. Weinstein RS, Nicholas RW, Manolagas SC. Apoptosis of osteocytes in glucocorticoid-induced osteonecrosis of the hip. J Clin Endocrinol Metab. 2000; 85:2907–2912. [PubMed: 10946902]
19. Roelofs AJ, Coxon FP, Ebetino FH, Lundy MW, Henneman ZJ, Nancollas GH, Sun S, Blazewska KM, Bala JL, Kashemirov BA, Khalid AB, McKenna CE, Rogers MJ. Fluorescent risedronate analogues reveal bisphosphonate uptake by bone marrow monocytes and localization around osteocytes in vivo. J Bone Miner Res. 2010; 25:606–616. [PubMed: 20422624]
20. Qing H, Ardeshirpour L, Pajevic PD, Dusevich V, Jahn K, Kato S, Wysolmerski J, Bonewald LF. Demonstration of osteocytic perilacunar/canalicular remodeling in mice during lactation. J Bone Miner Res. 2012:27.
21. Bellido T, Ali AA, Gubrij I, Plotkin LI, Fu Q, O'Brien CA, Manolagas SC, Jilka RL. Chronic elevation of parathyroid hormone in mice reduces expression of sclerostin by osteocytes: a novel mechanism for hormonal control of osteoblastogenesis. Endocrinology. 2005; 146:4577–4583. [PubMed: 16081646]
22. Weinstein RS, Jilka RL, Almeida M, Roberson PK, Manolagas SC. Intermittent parathyroid hormone administration counteracts the adverse effects of glucocorticoids on osteoblast and osteocyte viability, bone formation, and strength in mice. Endocrinology. 2010; 151:2641–2649. [PubMed: 20410195]

23. Nakanishi R, Akiyama H, Kimura H, Otsuki B, Shimizu M, Tsuboyama T, Nakamura T. Osteoblast-targeted expression of Sfrp4 in mice results in low bone mass. J Bone Miner Res. 2008; 23:271–277. [PubMed: 17907918]
24. Kamiya N, Ye L, Kobayashi T, Mochida Y, Yamauchi M, Kronenberg HM, Feng JQ, Mishina Y. BMP signaling negatively regulates bone mass through sclerostin by inhibiting the canonical Wnt pathway. Development. 2008; 135:3801–3811. [PubMed: 18927151]
25. Pederson L, Ruan M, Westendorf JJ, Khosla S, Oursler MJ. Regulation of bone formation by osteoclasts involves Wnt/BMP signaling and the chemokine sphingosine-1-phosphate. Proc Natl Acad Sci U S A. 2008; 105:20764–20769. [PubMed: 19075223]
26. Giraudo E, Inoue M, Hanahan D. An amino-bisphosphonate targets MMP-9-expressing macrophages and angiogenesis to impair cervical carcinogenesis. J Clin Invest. 2004; 114:623–633. [PubMed: 15343380]
27. Lai KA, Shen WJ, Yang CY, Shao CJ, Hsu JT, Lin RM. The use of alendronate to prevent early collapse of the femoral head in patients with nontraumatic osteonecrosis. A randomized clinical study. J Bone Joint Surg Am. 2005; 87:2155–2159. [PubMed: 16203877]
28. Drake MT, Srinivasan B, Modder UI, Ng AC, Undale AH, Roforth MM, Peterson JM, McCready LK, Riggs BL, Khosla S. Effects of intermittent parathyroid hormone treatment on osteoprogenitor cells in postmenopausal women. Bone. 2011; 49:349–355. [PubMed: 21600325]
29. Rossini M, Adami S, Viapiana O, Fracassi E, Ortolani R, Vella A, Zanotti R, Tripi G, Idolazzi L, Gatti D. Long-Term Effects of Amino-Bisphosphonates on Circulating gammadelta T Cells. Calcif Tissue Int. 2012; 91:395–399. [PubMed: 23052225]
30. Meraviglia S, Eberl M, Vermijlen D, Todaro M, Buccheri S, Cicero G, La Mendola C, Guggino G, D'Asaro M, Orlando V, Scarpa F, Roberts A, Caccamo N, Stassi G, Dieli F, Hayday AC. In vivo manipulation of Vgamma9Vdelta2 T cells with zoledronate and low-dose interleukin-2 for immunotherapy of advanced breast cancer patients. Clin Exp Immunol. 2010; 161:290–297. [PubMed: 20491785]
31. Rossini M, Adami S, Viapiana O, Ortolani R, Vella A, Fracassi E, Gatti D. Circulating gammadelta T cells and the risk of acute-phase response after zoledronic acid administration. J Bone Miner Res. 2012
32. Weinstein RS, Roberson PK, Manolagas SC. Giant osteoclast formation and long-term oral bisphosphonate therapy. N Engl J Med. 2009; 360:53–62. [PubMed: 19118304]
33. Coxon FP, Thompson K, Rogers MJ. Recent advances in understanding the mechanism of action of bisphosphonates. Curr Opin Pharmacol. 2006; 6:307–312. [PubMed: 16650801]
34. Halasy-Nagy JM, Rodan GA, Reszka AA. Inhibition of bone resorption by alendronate and risedronate does not require osteoclast apoptosis. Bone. 2001; 29:553–559. [PubMed: 11728926]
35. Ferguson VL, Ayers RA, Bateman TA, Simske SJ. Bone development and age-related bone loss in male C57BL/6J mice. Bone. 2003; 33:387–398. [PubMed: 13678781]
36. CDER. Pharmacology and Toxicology, Guidance for Industry, Estimating the Maximum Safe Starting Dose in Initial Clinical Trials for Therapeutics in Adult Healthy Volunteers. 2005.

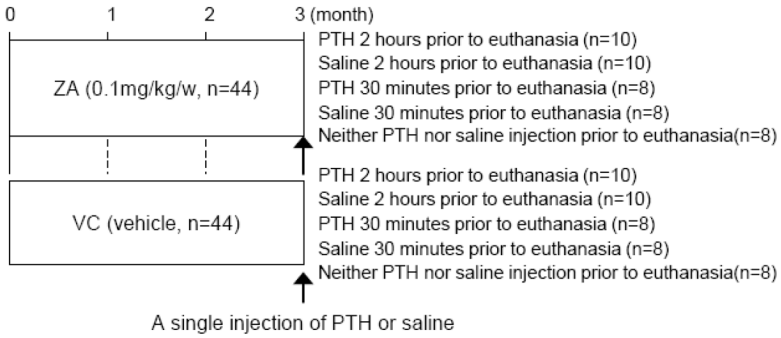

Fig 1.

Experimental schedule. A single injection of PTH or saline was performed 30 minutes or 2 hours before euthanasia to determine the effect of 3-month ZA treatment on osteocytes' responses to acute PTH.

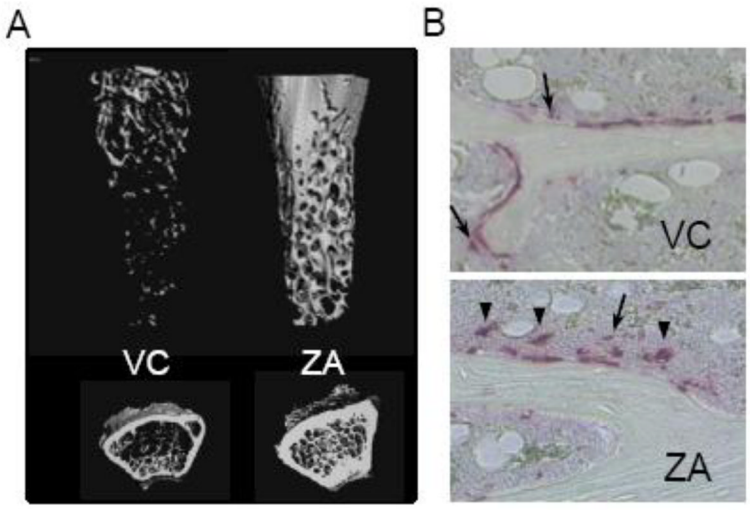

Fig 2.

A, Representative 3D reconstructions of the metaphyseal trabecular bone of the distal femurs. B, Representative photomicrographs of TRAP-stained trabecular bone sections show non-attached osteoclasts (arrow head) and $TRAP^{+}$ MNCs (arrow) near the bone surfaces.

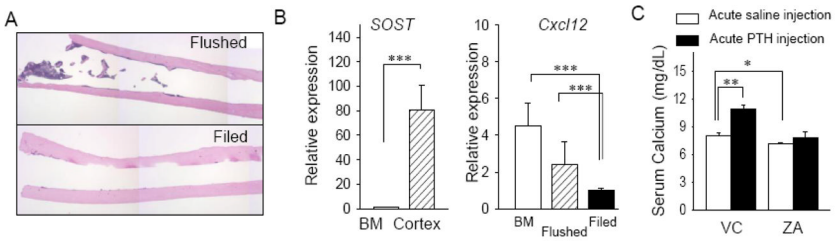

Fig 3.

Isolation of osteocyte dominant RNA. A, Representative photomicrographs of H&E-stained sections of the tibiae where a bone flush (top) and filing technique (bottom) were used. Remnants of the BM was obvious in the flushed tibia but not in the filed tibia. B, Total RNA was isolated from the filed cortical bone and qPCR performed to verify osteocyte dominant RNA by evaluating *SOST* and BM dominant RNA by assessing *cxcl12* expression. C, Serum calcium levels at 12 weeks were plotted. 3-month ZA-treatment significantly decreased the serum calcium levels. A single injection of PTH increased the serum calcium levels significantly in the VC-treated mice but not in the ZA-treated mice. n>5/group, $^{*}P < 0.05$, $^{**}P < 0.01$, $^{***}P < 0.001$.

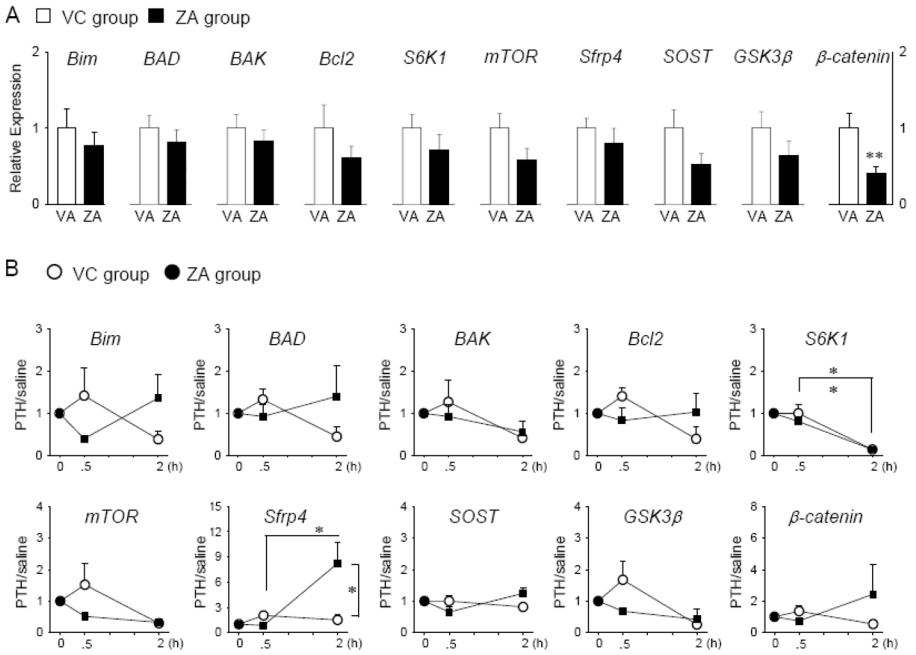

Fig 4.

ZA treatment influenced the gene expression of osteocytes in responses to acute PTH. Total RNA was isolated from the filed tibial cortex and qPCR was performed. Results normalized to *GAPDH* are presented. Apoptosis-related genes (*Bim*, *BAD*, *BAK*, and *Bcl2*), cell proliferation (*S6K1* and *mTOR*), and Wnt signaling-related genes (*sfrp4*, *SOST*, *GSK3β*, and *β-catenin*) were analyzed. A, The effect of 3-months ZA and VC treatment on the gene expression of osteocytes were assessed. B, The osteocytes' responses to acute PTH over acute saline were plotted for mice on 3-month VC and ZA treatment. The value in the plot is greater than one when acute PTH upregulated the gene expression of osteocytes. n=5/group, $^{*}P < 0.05$

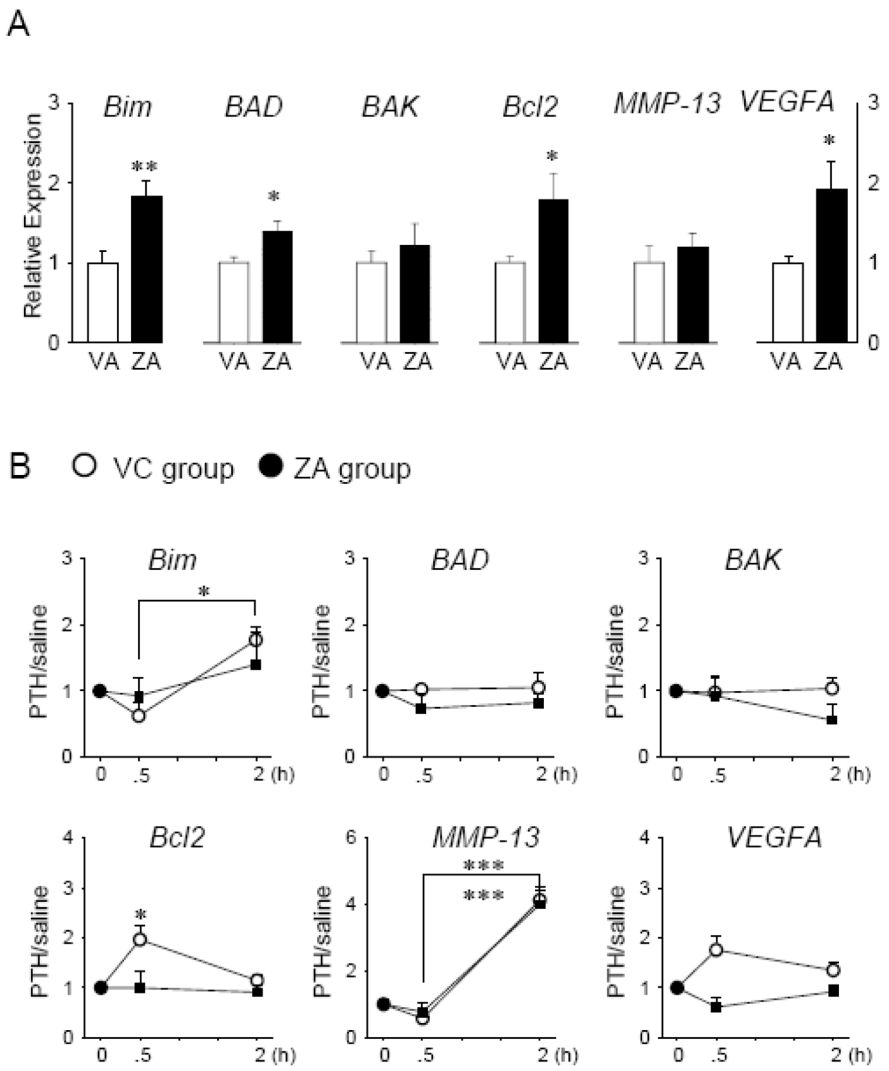

Fig 5.

ZA treatment influenced the gene expression of BM cells in response to acute PTH. Total RNA was isolated and qPCR was performed. Results normalized to *GAPDH* are presented. Apoptosis-related genes (*Bim*, *BAD*, *BAK*, and *Bcl2*), *MMP-13*, and *VEGFA* were analyzed. A, The effect of 3-months ZA and VC treatment on the gene expression of the BM were assessed. B, The responses of the BM to acute PTH over saline were plotted for mice on 3-month VC and ZA treatment. The value in the plot is greater than one when acute PTH upregulated the gene expression of the BM. n=5/group, $^{*}P < 0.05$, $^{**}P < 0.01$, $^{***}P < 0.001$

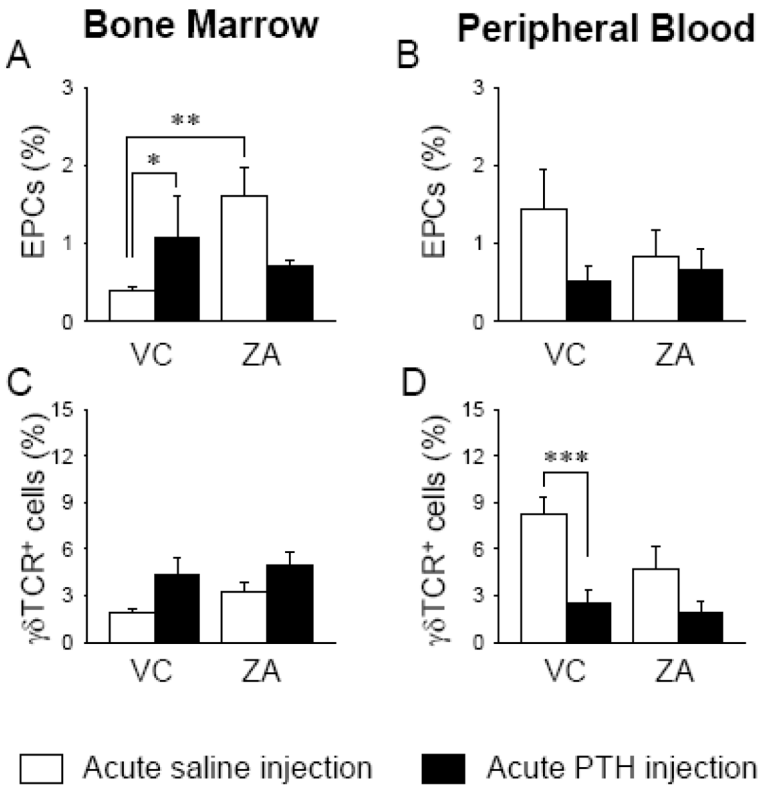

Fig 6.

ZA treatment increased $CD34^+CD133^+VEGFR2^+$ EPCs significantly in the BM (A) but not in PB (B). Acute PTH increased EPCs in the BM of the VC- treated but not in ZA-treated mice (A). In the VC-treated mice, acute PTH had no effect on γδT-cells in the BM (C) but significantly suppressed in PB (D). However, in ZA-treated mice no effects were observed in both VC- and ZA-treated mice. n=10/group, $^*P < 0.05$, $^{**}P < 0.01$, $^{***}P < 0.001$

Table 1

Primers used for quantitative real-time PCR

Gene	Accession number	Forward (5′-3′)	Reverse (5′-3′)
GAPDH	NM_008084.2	ACCCAGAAGACTGTGGATGG	CACATTGGGGGTAGGAACAC
18S	NR_003278.1	TTGACGGAAGGGCACCACCAG	GCACCACCACCCACGGAATCG
Bcl2	NM_009741.3	GGTCTTCAGAGACAGCCAGG	GATCCAGGATAACGGAGGCT
BAD	NM_007522.2	GTACGAACTGTGGCGACTCC	GAGCAACATTCATCAGCAGG
BAK	NM_007523.2	TATTAACCGGCGCTACGACAC	CTTAAATAGGCTGGAGGCGATCTT
Bim	NM_207680.2	CGACAGTCTCAGGAGGAACC	CCTTCTCCATACCAGACGGA
mTOR	NM_020009.2	CTCAGGCTGCTGGAGCTTAT	GCCAAAGCACTGCACTACAA
S6K1	NM_001114334.1	GAATGTTCCGCTCTGCTTTC	CTGGGAAGATATTTGCCATGA
β-catenin	NM_007614.3	CCCAGTCCTTCACGCAAGAG	CATCTAGCGTCTCAGGGAACA
GSK3β	NM_019827.6	GTGGTTACCTTGCTGCCATC	GACCGAGAACCACCTCCTTT
SOST	NM_024449.5	AGCCTTCAGGAATGATGCCAC	CTTTGGCGTCATAGGGATGGT
Sfrp4	NM_016687.3	AGAAGGTCCATACAGTGGGAAG	GTTACTGCGACTGGTGCGA
VEGFA	NM_001025250.3	AATGCTTTCTCCGCTCTGAA	GCTTCCTACAGCACAGCAGA
MMP-13	NM_008607.2	GGTCCTTGGAGTGATCCAGA	TGATGAAACCTGGACAAGCA
Cxcl12	NM_021807.3	GAGCCAACGTCAAGCATCTG	CGGGTCAATGCACACTTGTC

Table 2

Bone Histomorphometry and serum chemistry

Parameter	Vehicle Control (VC)	Zoledronate (ZA)
Trabecular bone		
BV/TV (%)	9.3 ± 1.3	71.8 ± 1.0***
Tb.N (1/mm)	3.7 ± 0.1	7.8 ± 0.2***
Tb.Th (μm)	47.2 ± 1.9	122.5 ± 1.2***
Tb.Sp (μm)	264.7 ±11.3	99.4 ± 9.9***
Conn.D. (1/mm^3)	60.3 ± 11.7	124.7 ± 18.7*
TMD (mg/cc)	792.9 ± 15.3	845.2 ± 10.0*
Cortical bone		
Ct.Th (mm)	1.88 ± 0.05	2.12 ± 0.05*
Porosity (%)	7.6 ± 0.1	5.4 ± 0.1***
TMD (mg/cc)	1210.7 ± 6.0	1254.7 ± 7.3**
Histomorphometry		
Ob.S/BS (%)	6.0 ± 0.7	6.8 ± 0.8
Oc.S/BS (%)	25.2 ± 1.9	17.9 ± 1.0**
Oc.N/BS (#/mm)	8.3 ± 0.5	3.7 ± 0.3***
Oc size (μm)	24.7 ± 1.7	39.5 ± 1.4***
Non-attached Oc (#/mm^2)	7.7 ± 1.6	40.5 ± 4.9***
TRAP$^+$ MNCs (#/mm^2)	6.1 ± 1.4	26.6 ± 3.4***
Serum TRAcP 5b (U/L)	7.41 ± 0.97	5.13 ± 0.39*

n > 7/group.

* $P < 0.05$,

** $P < 0.01$.

*** $P < 0.001$.